RSC Advances

PAPER

View Article Online
View Journal | View Issue

Cite this: *RSC Adv.*, 2020, **10**, 38085

The design and synthesis of high efficiency adsorption materials for 1,3-propanediol: physical and chemical structure regulation†

Kexin Zheng,‡[ab] Long Jiang,‡[b] Shitao Yu,[a] Mo Xian,[b] Zhanqian Song,[ac] Shiwei Liu*[a] and Chao Xu *[b]

Received 15th July 2020
Accepted 1st October 2020

DOI: 10.1039/d0ra06167k

rsc.li/rsc-advances

In this study, a series of polystyrene-divinylbenzene resins with precise physical structure regulation and chemical modification were successfully synthesized. The regulation of Friedel–Crafts reaction conditions resulted in several physical resins with various BET surface areas and pore structures, while the adsorption of 1,3-propanediol revealed that the molecular size and other physical properties exhibited a moderate contribution to the adsorption of hydrophilic compounds. The adsorption processes between 1,3-propanediol and nitrogen, oxygen and boron functional group modified resins were further explored, and boronic acid modified resins named PS-3NB and PS-SBT exhibited higher adsorption capacities than commercial resin CHA-111. The adsorption capacity of PS-3NB and PS-SBT reached 17.54 mg g^{-1} and 17.23 mg g^{-1}, respectively, which were 37% and 35% higher than that of commercial resin CHA-111. Furthermore, the adsorption mechanism demonstrated that the content of boronic acid, solution pH and adsorbate hydrophobicity were the primary adsorption driving forces. Herein, we provided a method to modify polystyrene-divinylbenzene materials with boronic acid to selectively adsorb hydrophilic polyols *via* the specific affinity between boronic acid and diol molecule.

1 Introduction

Polyols including glycerol, 1,3-propanediol and 1,2-butanediol are important raw materials and intermediates in pharmaceuticals, chemicals, food and other fields.[1] Currently, the environmentally friendly fermentative polyols have been widely applied, and the separation and purification of them has been an important research field in chemistry.[2–4] However, the high boiling point and strong hydrophilicity restrict the development of related separation technologies.

In recent years, distillation and membrane separation are commonly used to separate polyols from fermentation broth or aqueous media. The traditional distillation method[5] has been used to separate 1,2-propanediol, 1,3-propanediol, *etc.*, while the key problem is the relatively high boiling point resulting in high energy consumption and high cost. Membrane separation method[6,7] can be used to separate and purify polyols from biological fermentation broth and biodiesel, but the membrane service life, effective membrane retention capacity and membrane fouling limit the practical application. As an efficient and green separation method, adsorption has attracted more and more attention with the advantages of low cost, low pollution and reproducibility.

Currently, the commonly utilized adsorbents are activated carbon,[8,9] zeolite,[10–12] silica gel[13,14] and adsorption resin.[15,16] Adsorption resin has attracted extensive attention due to their high specific surface area, adjustable pore structure and stable mechanical strength.[17] In the early 1970s, Davankov first reported the synthesis of hyper-crosslinked polystyrenes resin.[18] Hyper-crosslinked resin as a physical regulated resin owns high specific surface area and rich pore diameter structure, which has been widely used in the adsorption and separation of phenols,[19,20] anilines,[21–23] dyes[24] and other substances. Besides, the introduction of chemical functional groups on resin skeleton can improve the surface properties of resins, exhibiting good adsorption and separation performance for phenols,[25–27] amines[28–30] and other substances. However, there are few reports on the selective adsorption of polyols by adjusting the physical or chemical structure of resin. Therefore, it is necessary to study the effects and mechanisms of physical structure regulation and chemical modification on the adsorption and separation of polyols.

[a]*Chemical Engineering and Technology, Qingdao University of Science & Technology, Qingdao 266042, China. E-mail: liushiweiqust@126.com; Tel: +86-0532-8402-2782*
[b]*Key Laboratory of Biobased Materials, Qingdao Institute of Bioenergy and Bioprocess Technology, Chinese Academy of Sciences, Qingdao 266101, China. E-mail: xuchao@qibebt.ac.cn; Tel: +86-0532-5878-2981*
[c]*National Engineering & Technology Research Center of Forest Chemical Industry, Institute of Chemical Industry of Forest Products, Chinese Academy of Forestry, Nanjing 210042, China*

† Electronic supplementary information (ESI) available. See DOI: 10.1039/d0ra06167k

‡ These authors contributed equally to this work.

In our previous study,[16] we proved that it is feasible to introduce boronic acid functional group into chloromethyl sites of CMPS to realize polyol adsorption. However, the in-depth studies on the influence of physical structure regulation and chemical functional modification to the adsorption of polyol and the rational utilization of chloromethyl sites remained to be explored. In this study, a series of physical structure regulated and nitrogen, oxygen, boron functional groups modified resins were synthesized with chloromethyl polystyrene-divinylbenzene as precursor. 1,3-Propanediol was taken as the research object, and the influences of adsorption capacity and pore structure, specific surface area, functional group, pH, temperature and other factors were deeply explored.

2 Experimental

2.1 Materials

Chloromethyl styrene divinylbenzene (CMPS), with cross-linking degree of 7% and chlorine content of 18.9%, was purchased from Zhengzhou Diligent Technology Co. Ltd. Commercial resin CHA-111 was obtained from Zhengzhou High-Tech Technology Co. Ltd. Gallic acid (GA), ethylenediamine (EDA), cesium carbonate ($CsCO_3$), sodium periodate ($NaIO_4$), 4-carboxyphenylboronic acid (SB), 4-carboxylphenylboronic acid pinacol ester (SBZ), 4-aminophenylboronic acid pinacol ester (NBZ), 3-aminophenylboronic acid pinacol ester (3NBZ), 3-aminophenylboronic acid (3NB) and 4-hydroxyphenylboronic acid pinacol ester (OBZ) in AR grade were purchased from Aladdin Chemical Reagent Co. Ltd. Nitrobenzene (NB), anhydrous aluminum chloride, *N*,*N*-dimethylformamide (DMF), potassium carbonate (K_2CO_3), sodium bicarbonate ($NaHCO_3$), ammonium chloride (NH_4Cl), sodium hydroxide, hydrochloric acid, methanol (MeOH), ethanol and 1,3-propanediol (1,3-PD) were purchased from Sinopharm Chemical Reagent Co. Ltd. All reagents were AR grade, without further purified.

2.2 Synthesis of resins

2.2.1 Synthesis of physical structure regulated resins. The physical structure regulated resins were synthesized under different temperature and reaction time on basis of CMPS in nitrobenzene *via* anhydrous aluminum chloride as catalyst. Precursor resin CMPS were subjected to the specified temperature (40 °C, 80 °C, 100 °C, 120 °C and 135 °C) for 4 h to obtain the resins. Under ultrasonic conditions, the resins were cleaned with ethanol and deionized water for several times and dried at 70 °C for 24 h, which were named as PS-W40, PS-W80, PS-W100, PS-W120 and PS-W135 resins. CMPS were subjected to 60 °C under various reaction times (0.5 h, 1 h, 4 h, 8 h and 12 h) to generate PS-S0.5, PS-S1, PS-S4, PS-S8 and PS-S12 resins (the synthesis method was shown in ESI Section 1.1†).

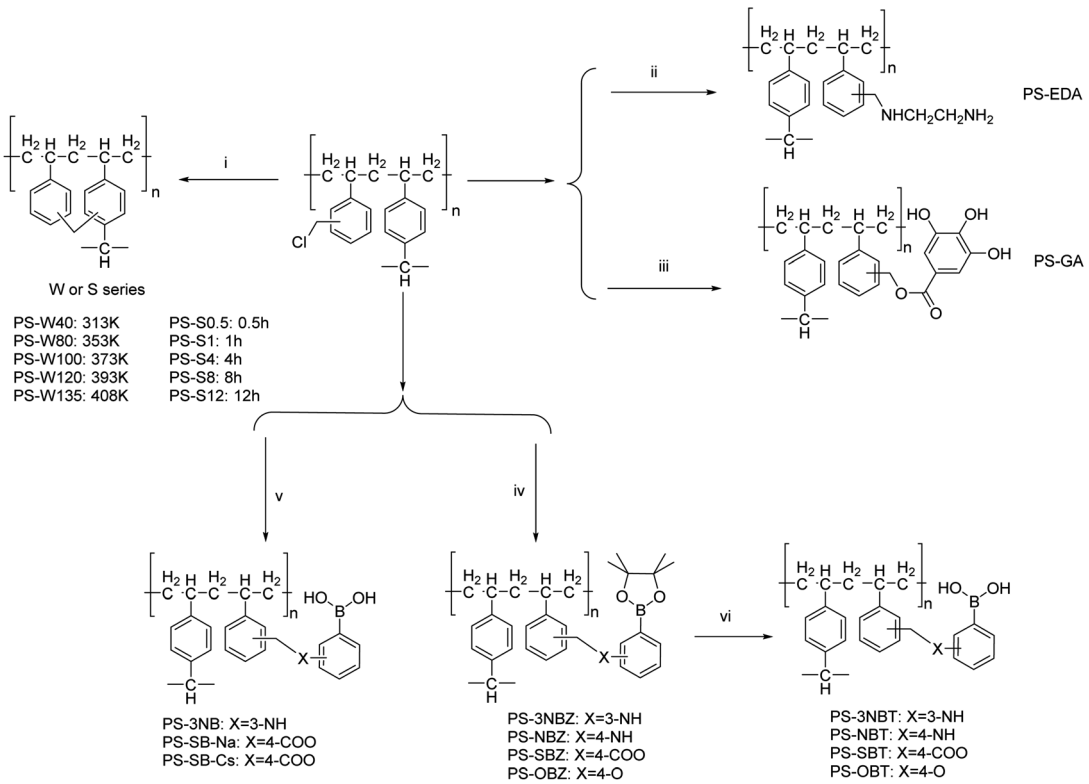

Reagents and conditions: (i) NB,$AlCl_3$,Heat;(ii) DMF,K_2CO_3,EDA,353K,24h;(iii) DMF,$NaHCO_3$,GA,353K,24h ;(iv)and (v) DMF,$NaHCO_3$ or $CsCO_3$,353K,24h; (vi) MeOH,NH_4Cl,$NaIO_4$,298K,18h.

Scheme 1 Synthesis of physical and chemical modified resins.

2.2.2 Synthesis of chemical functional group modified resins. The synthesis method of PS-EDA and PS-GA modified resin was shown in ESI Section 1.2.† PS-EDA modified resin was prepared by amination reaction of CMPS and DMF with ethylenediamine under the action of alkali K_2CO_3, which was similar to gallic acid modified resin and boronic acid modified resins. PS-GA modified resin was prepared by esterification of CMPS with gallic acid under the action of strong base $NaHCO_3$ (Scheme 1).

Synthesis of boronic acid modified resins: a series of boronic acid modified resins were synthesized by the method shown in ESI Section 1.2.† PS-SB and PS-SBZ modified resins were prepared by nucleophilic substitution reaction of CMPS with boronic acid under the action of strong base $NaHCO_3$ or $CsCO_3$. The deprotection scheme of PS-SBZ boronic acid pinacol ester modified resins were employed $NaIO_4$ to remove the protection group to obtain PS-SBT resins. Detailed synthesis conditions were shown in Table 1.

2.3 Adsorption experiments

2.3.1 Batch adsorption. Static adsorption experiments were carried out in 10 mL centrifuge tubes with 0.02 g resins and 1 mL 1,3-propanediol with an initial concentration of 2 g L^{-1} (except thermodynamic experimental study). The different pH of the solution was adjusted by NaOH or HCl and then shaken in a thermostatic oscillator at a desired temperature with the rotation speed at 180 rpm for 16 h. The equilibrium concentration was determined by HPLC-RID (high performance liquid chromatography with refractive index detector, Agilent Technologies lnc., Santa Clara, California, USA). The adsorption capacity was calculated by the following formula:

$$Q_e = V(C_0 - C_e)/M \quad (1)$$

where Q_e (mg g^{-1}) is the equilibrium adsorption capacity; C_0 (mg L^{-1}) is the initial concentration of adsorbate in the solution; C_e (mg L^{-1}) is the equilibrium concentration in the solution; V (L) is the volume of adsorbate solution; M (g) is the mass of the resin.

Table 1 Reaction conditions of chemical modified resins

Resin	Precursor resin	Functional group	Reaction conditions
PS-EDA	CMPS	EDA	DMF/K_2CO_3/353 K/24 h
PS-GA	CMPS	GA	DMF/$NaHCO_3$/353 K/24 h
PS-SB-Na	CMPS	SB	DMF/$NaHCO_3$/353 K/24 h
PS-SB-Cs	CMPS	SB	DMF/$CsCO_3$/353 K/24 h
PS-3NB	CMPS	3NB	DMF/$CsCO_3$/353 K/24 h
PS-3NBZ	CMPS	3NBZ	DMF/$CsCO_3$/353 K/24 h
PS-NBZ	CMPS	NBZ	DMF/$CsCO_3$/353 K/24 h
PS-OBZ	CMPS	OBZ	DMF/$CsCO_3$/353 K/24 h
PS-SBZ	CMPS	SBZ	DMF/$NaHCO_3$/353 K/24 h
PS-3NBT	PS-3NBZ	3NBT	$NaIO_4$/MeOH/NH_4Cl/298 K/18 h
PS-NBT	PS-NBZ	NBT	$NaIO_4$/MeOH/NH_4Cl/298 K/18 h
PS-OBT	PS-OBZ	OBT	$NaIO_4$/MeOH/NH_4Cl/298 K/18 h
PS-SBT	PS-SBZ	SBT	$NaIO_4$/MeOH/NH_4Cl/298 K/18 h

2.3.2 Competitive adsorption. Competitive adsorption experiments were carried out in 10 mL centrifuge tubes with 0.02 g resins and 1 mL adsorbate with an initial concentration of 2 g L^{-1} (the adsorbates were two-component mixed systems of 1,3-propanediol and glycol, glycerol, 1,2-butanediol, 1,3-butanediol, 1,4-butanediol and catechol, respectively. And the pH of mixed systems solution was 10). The pH of the solution was adjusted by NaOH or HCl and adsorption process at 298 K for 16 h. The equilibrium concentration was determined by HPLC-RID. The adsorption capacity was calculated by the formula (1).

2.3.3 Thermodynamic study. Thermodynamic study was conducted with different initial concentration of 1,3-propanediol from 1 to 24 g L^{-1} (1, 4, 8, 12 and 24 g L^{-1}) at 293 K, 303 K and 313 K and 180 rpm for 16 h. The adsorption capacity was calculated by the formula (1). The Langmuir and Freundlich models were applied to further investigate the thermodynamics of PS-SBT and commercial resin CHA-111. The Langmuir and Freundlich model equation are exhibited by formula (2) and (3):[16,24]

$$Q_e = C_e K_L Q_m/(1 + K_L C_e) \quad (2)$$

$$Q_e = K_F C_e^{1/n} \quad (3)$$

where Q_e (mg g^{-1}) is the equilibrium adsorption capacity; Q_m (mg g^{-1}) is the maximum adsorption capacity; C_e (g L^{-1}) is the equilibrium concentration in the solution; K_L (L g^{-1}), K_F (mg^{1-n}) and n corresponding characteristic constants.

2.3.4 Desorption and regeneration. After adsorption completed, an equal volume of 0.1 mol L^{-1} hydrochloric acid was added for desorption. The desorption experiment temperature was set at 298 K for 24 h. The resin was washed in ethanol and deionized water until neutral, and then dried in air dry oven at 323 K for 12 h for the next adsorption.

2.3.5 Analysis. The resins were characterized by Fourier Transform Infrared Spectroscopy (FT-IR Nicolet iN10 IR Microscope) from 500–4000 cm^{-1}. BET surface area and pore volume were measured by N_2 adsorption–desorption with ASAP 2020 (Micromeritics) at 77 K. BET surface area was calculated by single point BET method model fitting, and the distribution of pore diameter was obtained by original density functional theory (DFT) equation simulation. The concentration of adsorbate solution was determined by HPLC-RID (high performance liquid chromatography with refractive index detector, Agilent Technologies lnc., Santa Clara, California, USA). The thermal stability of the resin was determined by a synchronous thermogravimetric-differential scanning calorimeter (STA449F5 jupiter, USA). The XPS was characterized by ThermoFisher (ESCALAB Xi+, USA).

The residual chlorine content of resin was determined by Volhard method.[46] The specific determination method as follows: accurately weighed 0.2 g resin into the crucible and added 1 g NaOH and 1 g KNO_3 to stir evenly, then covered the surface with a layer of KNO_3, put the crucible in muff furnace and decomposed it under 873 K for 4 h. After the muff furnace being cooled to room temperature, the sample was taken out,

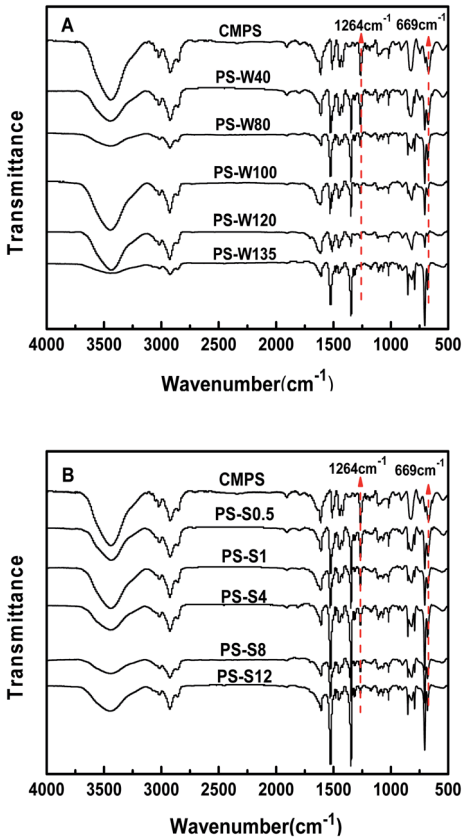

Fig. 1 IR spectra (wavenumbers from 500–4000 cm^{-1}) of PS-W and PS-S series physical resins (A and B).

dissolved in pure water and then added phenolphthalein indicator. Added concentrated nitric acid into the system to adjust pH to acidity and 2 mL nitrobenzene to protect chloride ion. After adding an excess of 0.1 M silver nitrate standard solution and alum iron as an indicator, titrate with potassium thiocyanate standard solution and the chlorine content was calculated. The boronic acid content of boronic acid modified resins were determined by titration method (ESI Section 2†).

3 Results and discussion

3.1 Physical structure regulated resins

3.1.1 Characterization of the physical structure regulated resins. Based on the regulation of Friedel–Craft reaction time and temperature, a series of physical structure regulated resins named PS-W40–PS-W135 and PS-S0.5–PS-S12 were synthesized. As the FT-IR results shown in Fig. 1A, the C–Cl vibration bands of PS-W40–PS-W135 resins at 1264 cm^{-1} and 669 cm^{-1} decreased significantly with the increase of the reaction temperature.[31] Besides, Fig. 1B showed the characteristic peak of C–Cl on PS-S0.5–PS-S12 series resins decreased with the increase of reaction time. Hence, the reduced chloromethyl vibration could qualitatively show the extent of the Friedel–Craft reaction, and PS-W135 and PS-S12 nearly completely consumed the chloromethyl.

In order to further study the residual chlorine content of PS-W and PS-S series resins, Volhard method was employed for quantitative determination (Fig. 2A and B). There were 18.9%, 12.9% and 1.8% residual chlorine in the precursor resin CMPS, PS-W40 and PS-W135, respectively, and the residual chlorine

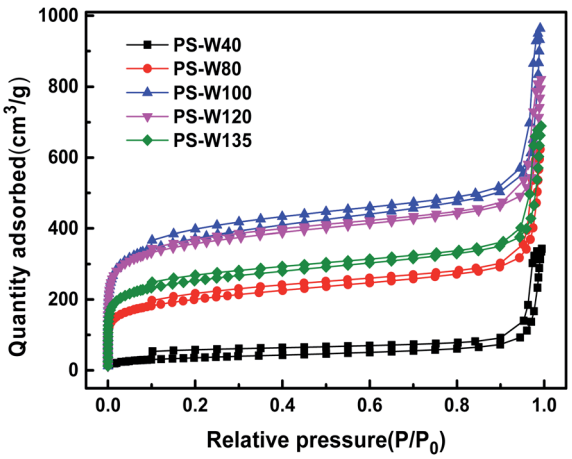

Fig. 3 N_2 adsorption–desorption curves of PS-W series physical resins.

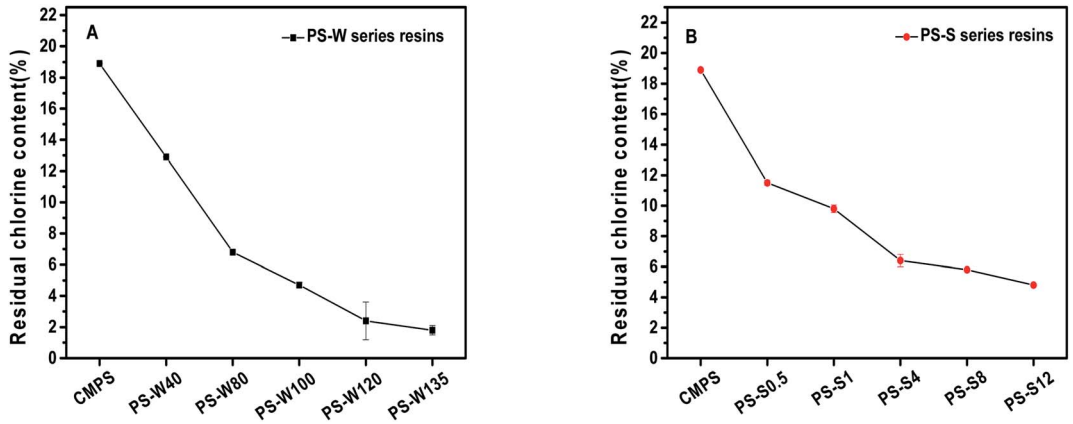

Fig. 2 The residual chlorine content of PS-W and PS-S series physical resins (A and B).

Table 2 The pore volume and BET surface area of CHA-111 and PS-W100 within 0–5 nm

Pore diameter (nm)		0–1	1–2	2–3	3–4	4–5	Total
BET ($m^2\ g^{-1}$)	CHA-111	443.8	360.4	58.2	23.7	11.4	1414.4
	PS-W100	494.2	300.9	34.4	9.3	3.7	1381.5
Volume ($cm^3\ g^{-1}$)	CHA-111	0.157	0.254	0.069	0.042	0.027	1.32
	PS-W100	0.180	0.204	0.038	0.016	0.009	0.86

curve of PS-W series resins decreased rapidly with the increase of temperature and then decreased slowly. Meanwhile, the residual chlorine content decreased from 11.5% to 4.8% as the reaction time increased from 0.5 h to 12 h, exhibiting an inverse relation with Friedel–Craft reaction time. It presented the increase of reaction temperature and time leaded to the rapid consumption of chloromethyl. Subsequently, the reaction was slowed down due to the increase of steric hindrance and the decrease of chloromethyl site, which was consistent with the FT-IR results. Hence, the PS-W and PS-S series physical structure regulated resins were successful synthesized.

The specific surface area and pore structure of PS-W and PS-S series resins are related to the adsorption capacity. High specific surface area and appropriate pore size are conducive to the adsorption of small molecule. As the N_2 physical adsorption–desorption shown in Fig. 3, the physical structure regulated resins owned obvious specific surface area advantage and abundant pore structure (Table 2). Both PS-W and PS-S series resins showed a sharp increase in nitrogen adsorption capacity when the relative pressure was low ($P/P_0 < 0.05$), indicating that there were quite a large proportion of micropores in the resin. At the same time, the adsorption branch and desorption branch on the nitrogen adsorption–desorption curve had obvious hysteresis loop, indicating the existence of resin mesopores. When the relative pressure was high ($P/P_0 > 0.95$), the nitrogen adsorption capacity also showed a sharp increase, indicating that some macropores still existed in the resin[26] (PS-S series N_2 adsorption–desorption attached figure and pore diameter distribution figure were shown in Fig. S1†). The specific surface area of the resin increases with the increase in micropores and mesopores, which provides a powerful physical force for the adsorption of 1,3-propanediol.

3.1.2 Adsorption behavior of physical structure regulated resins. As the physical structure regulated resins were precisely regulated with the comparative BET surface area and pore structure, PS-W and PS-S series resins were subjected to 1,3-propanediol solution to further evaluate the adsorption capacity. Fig. 4 showed the adsorption relationship of 1,3-propanediol by the physical structure regulated resins. The adsorption capacity of PS-W100 and PS-W120 reached to 11.67 and 10.70 mg g^{-1}, respectively, which were 91% and 83.4% adsorption capacity of the commercial resin CHA-111. It was attributed to good pore structure and high specific surface area (commercial resins CHA-111, PS-W100 and PS-W120 have specific surface areas of 1414.4, 1381.5 and 1336.1 $m^2\ g^{-1}$, and micropore volume of 0.3008, 0.3022 and 0.3187 $cm^3\ g^{-1}$). It indicated that appropriate pore structure and high specific surface area are conducive to adsorption, and molecular size effect accounts for a large proportion in adsorption force.[32]

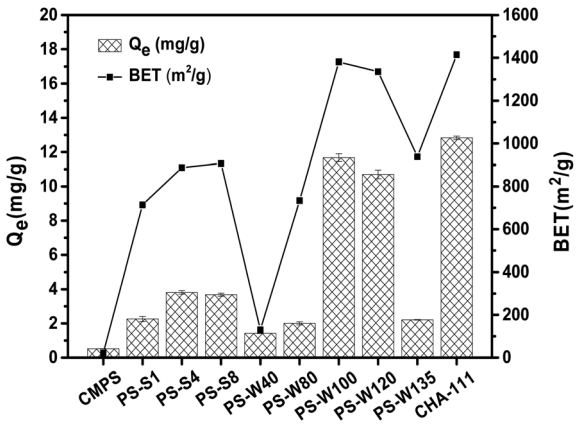

Fig. 4 Adsorption capacities for 1,3-propanediol and BET surface area of CMPS and physical resins (initial concentration 2 g L^{-1}, 30 °C, 16 h).

For small molecular organics such as *p*-aminobenzoic acid, micropores were more suitable for solute–solute interaction, Huang *et al.*[24] believed that the best match between the pore size of the resin and the molecular volume of the adsorbate was 2–6 times. According to the molecular size of 1,3-propanediol (0.74 × 0.48 × 0.42 nm, optimized simulation by software Gaussian 09W and Multiwfn), the optimal pore size of resin was 1.48–4.44 nm. Although the pore sizes of commercial resin CHA-111 and PS-W100 distributed at 1.48–4.44 nm have a high proportion of optimal adsorption pore diameter (Table 2), the considerable match between the pore size and molecule size failed to capture 1,3-propanediol. Therefore, the adsorption of 1,3-propanediol on the resin modified by different functional groups were further studied.

3.2 Chemical functional group modified resins

3.2.1 Characterization of chemical modified resins. In order to further investigate the adsorption of 1,3-propanediol on the modified resins of different functional groups, a series of nitrogen, oxygen and boron containing functional groups were introduced on the resin skeleton. As shown in Fig. 5A, the C–Cl vibration peaks of all the modified resins at 1264 cm^{-1} and 669 cm^{-1} were significantly weakened, indicating the chloromethyl active sites reacted adequately. The stretching vibration peak of ester carbonyl C=O appearing on PS-GA at 1730 cm^{-1}, and 1100 cm^{-1} was the stretching vibration peak of

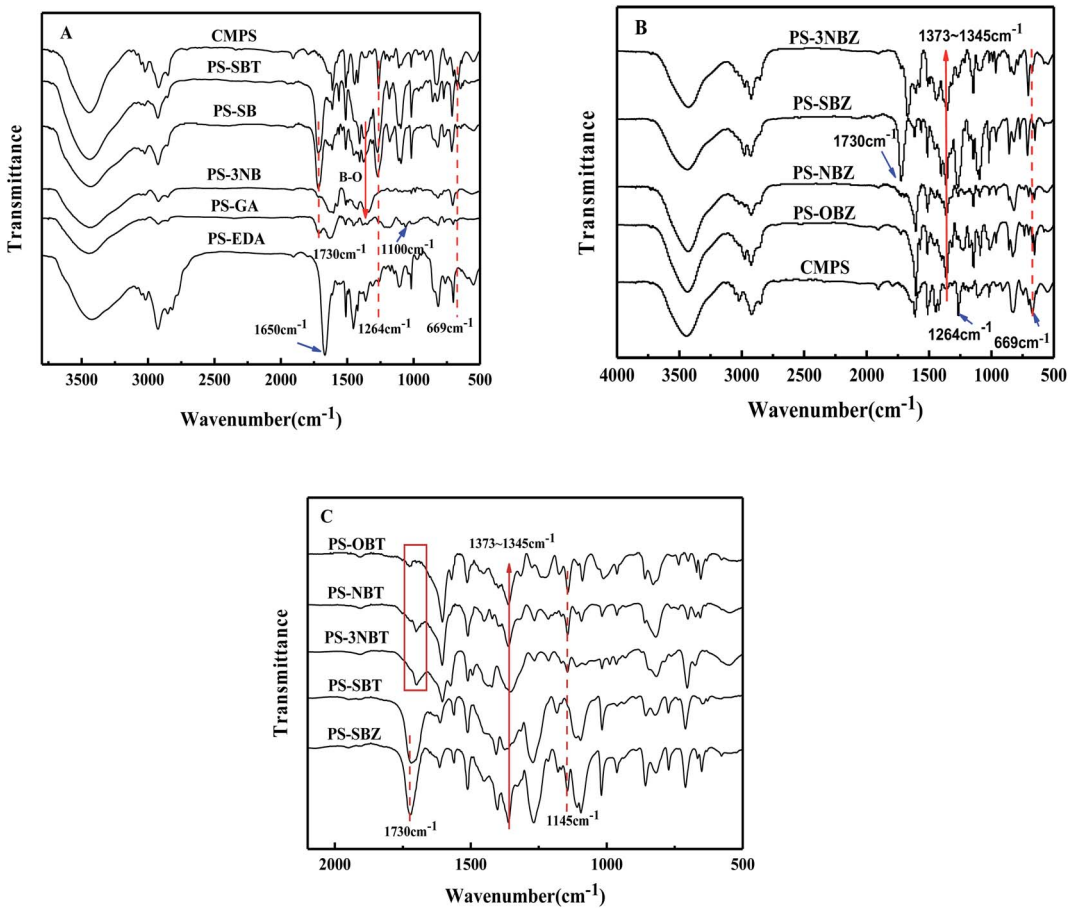

Fig. 5 IR spectra (wavenumbers from 500–4000 cm^{-1}) of modified resins with nitrogen, oxygen and boron functional groups (A), PS-SBZ type modified resins (B) and deprotection PS-SBT type modified resins (C).

C–O and bending vibration peak in the O–H plane, which preliminarily indicated that gallic acid has been successfully introduced.[33] In the PS-EDA spectrum of aminated resin, the stretching vibration peak of N–H bond appeared at 1650 cm^{-1},[34] indicating the success of amino modification. The characteristic peak of B–O bond appeared at 1373–1345 cm^{-1} of phenylboronic acid modified resins,[16] and the ester C=O stretching vibration peak appeared at 1730 cm^{-1} of 4-carboxylphenylboronic acid modified resins (PS-SB and PS-SBT), indicating that the modification was successful. In the PS-3NB spectra of 3-aminophenylboronic acid modified resin, the characteristic peak of N–H bond stretching vibration appeared at 1650 cm^{-1}, and the characteristic peak of B–O appeared at 1373–1345 cm^{-1}, indicating the successful modification of amination reaction. The boronic acid pinacol ester modified resins were characterized (Fig. 5B) and the C–Cl vibration peak strength of the four modified resins was greatly reduced. Besides, B–O bond characteristic peak appeared at 1373–1345 cm^{-1}, indicating the successful introduction of B–O bond of the four resins. Compared with the 4-carboxyphenylboronic acid modified resins (PS-SBZ and PS-SBT), the C–O–C characteristic peak at 1145 cm^{-1} had obviously decrease (Fig. 5C), indicating the usefulness of the deprotection scheme.[35] By infrared comparison of the other three modified resins, it was declared that the characteristic peak strength of C–O–C was not weakened, and unknown new peak appeared around 1700 cm^{-1} with the deprotection reaction, indicating that the three monomer modified resins' removal protection schemes had no obvious effect.

3.2.2 Adsorption behavior of chemical modified resins. According to the adsorption of 1,3-propanediol by the chemical modified resins (Fig. 6A), the nitrogen and oxygen functional groups modified resins showed moderate adsorption affinity. The adsorption capacity of gallic acid modified resin PS-GA and ethylenediamine modified resin PS-EDA were only 29.3% and 71.9% of that of CHA-111. The adsorption capacity of 4-carboxyphenylboronic acid modified resin PS-SBT and 3-aminophenylboronic acid modified resin PS-3NB reached to 17.23 and 15.67 mg g^{-1}, respectively, which was 35% and 22% higher than that of CHA-111 (12.83 mg g^{-1}). But the adsorption capacity of 4-aminophenylboronic acid modified resin PS-NBT and 4-hydroxyphenylboronic acid modified resin PS-OBT to 1,3-propanediol were less than 5 mg g^{-1}. It was worth mentioning that the usefulness of the 4-carboxyphenylboronic acid modified resin after pinacol ester protection scheme is also shown in the figure. The adsorption capacity of PS-SB-Na and PS-SB-Cs to 1,3-

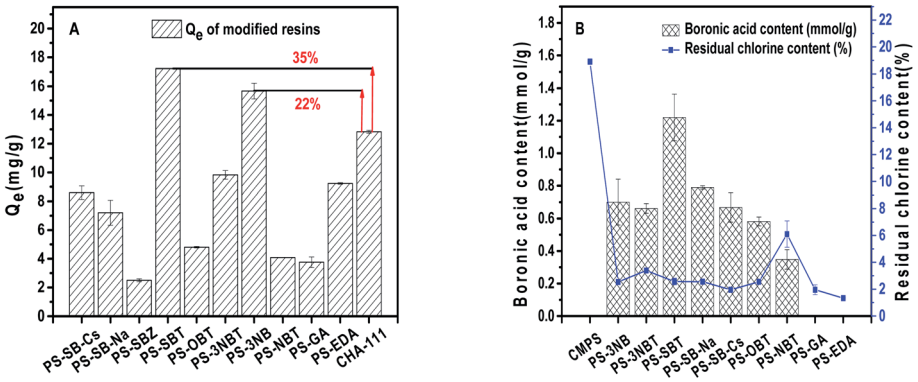

Fig. 6 Adsorption capacities of CHA-111 and chemical modified resins for 1,3-propanediol ((A) initial concentration 2 g L^{-1}, pH = 10, 30 °C, 16 h) and boronic acid loading capacity and residual chlorine content of chemical modified resins (B).

propanediol was 7.21 and 8.60 mg g^{-1}, respectively, only 41.8% and 49.9% of that of PS-SBT. The reason might be that different alkaline catalysts were employed in the synthesis process, which resulted in different chloromethyl sites being consumed. At the same time, PS-SBT introduced the pinacol ester protection hydroxyl group to reduce the adverse reaction of chloromethyl, and thus improving the content of boron functional group and increasing the adsorption capacity. It can be seen that the functional groups modified resins modified by different functional groups have different affinity for 1,3-propanediol, among which, the boron functional group modified resins can better adsorb 1,3-propanediol owe to the specific reaction of boronic acid and diol structure.[36]

3.3 Influence factors of adsorption

In order to study the influencing factors in the adsorption process of boronic acid modified resins, we further explored the effects of adsorbent loading boronic acid content, hydroxide ion concentration in aqueous media, temperature and other factors on adsorption.

3.3.1 Effect of loading boronic acid. In order to research the effect of boronic acid content in boronic acid modified resins on the adsorption of 1,3-propanediol, the boronic acid loading of the resin was calculated.[37,38] The quantitative analysis of the boronic acid loading in Fig. 6B showed that the 4-carboxyphenylboronic acid modified resin PS-SBT owned the highest 1.220 mmol g^{-1} boronic acid groups and consumed about 16% chloromethyl sites, which was superior to PS-SB-Cs (0.668 mmol g^{-1}) and PS-SB-Na (0.790 mmol g^{-1}). The boronic acid loading of PS-3NBT owned 0.662 mmol g^{-1}, which was inferior to PS-3NB (0.700 mmol g^{-1}). After protection, 3-aminophenylboronic acid modified resin did not increase the amount of introduction, which might be because the nucleophilicity of 3-aminophenylboronic acid pinacol ester was less than 3-amino phenylboronic acid and reduced the nucleophilic reaction efficiency per unit mass. The amount of boronic acid payload corresponded to the adsorption capacity, indicating that the higher the amount of boronic acid payload, the higher the adsorption capacity of 1,3-propanediol.

At the same time, the residual chloromethyl of modified resin was quantitatively calculated by Volhard method, and it was demonstrated that the chloromethyl content of boronic acid modified resins were 2–6%, and that of gallic acid PS-GA and amination resin PS-EDA were less than 2%. It indicates that the functional groups cannot react all chloromethyl sites in resin, which is mainly due to the large steric hindrance of the resin itself. The steric hindrance increases with the further

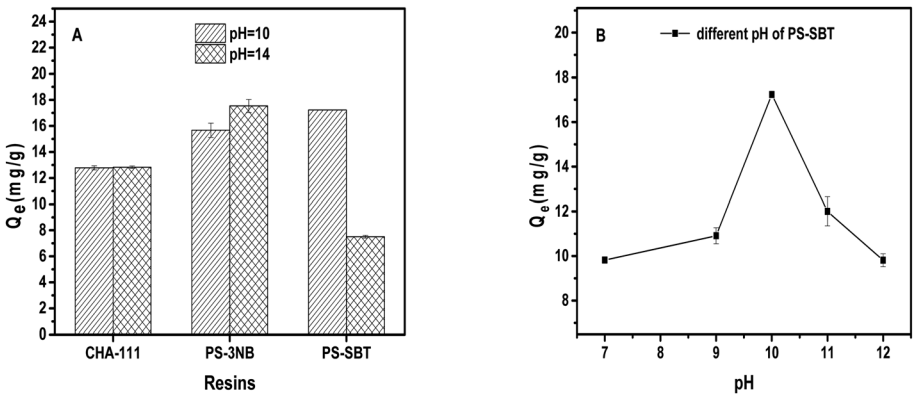

Fig. 7 Adsorption capacities of CHA-111 and boronic acid modified resins for 1,3-propanediol ((A) initial concentration 2 g L^{-1}, 30 °C, 16 h) and adsorption for 1,3-propanediol at different pH environments of PS-SBT ((B) initial concentration 2 g L^{-1}, 30 °C, 16 h).

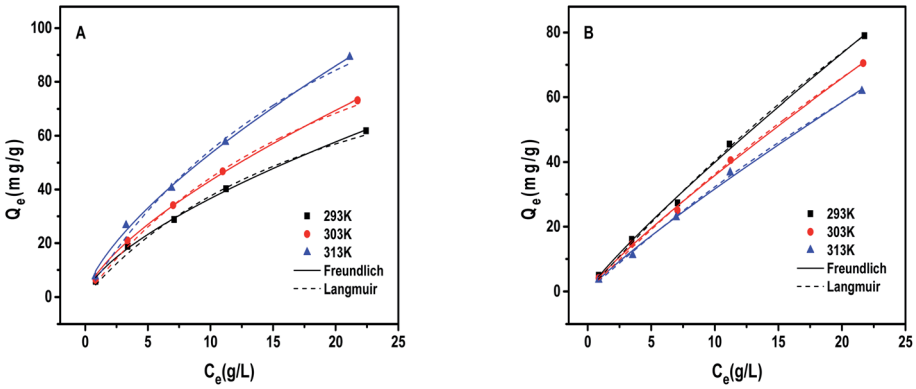

Fig. 8 Adsorption isotherm model of 1,3-propanediol with temperature at 293 K, 303 K and 313 K for boronic acid modified resin PS-SBT (A) and commercial resin CHA-111 (B), the initial concentration of 1,3-propanediol was set to be about 1, 4, 8, 12, and 24 g L^{-1}, pH = 10, 16 h.

introduction of functional monomer, which limits the reaction degree.

3.3.2 Effect of pH. Two boronic acid modified resins PS-SBT and PS-3NB showed different affinity with 1,3-propanediol in different pH environments. Fig. 7A showed that the adsorption capacity of PS-3NB increased with the increase of the alkalinity of the adsorbate, which was 122% and 137% of the commercial resin CHA-111 at pH were 10 and 14, respectively. However, the adsorption capacity of PS-SBT modified resin decreased with the increase of alkalinity of the adsorbate solution. When pH was 10, the adsorption capacity of PS-SBT was 135% of CHA-111, but decreased to 58.5% of CHA-111 when pH increased to 14. It is illustrated that PS-SBT may itself be unstable in a strong alkali environment,[39] and partial functional groups fall off, which destroys the excellent structure of the modified resin. Fig. 7B showed the variation trend of the adsorption capacity of 1,3-propanediol by PS-SBT resin at different pH values. The adsorption capacity increased with the increase of pH value, but decreased when the pH value was greater than 10. It indicated that the increase of pH was conducive to adsorption, and the affinity between boronic acid group and 1,3-propanediol was the best when pH = 10. Therefore, PS-SBT and PS-3NB resins were found to be stable in pH = 10 and 14,[16] respectively, with better adsorption effect.

3.3.3 Adsorption isotherm and thermodynamics. The adsorption behaviors of boronic acid modified resin PS-SBT at various temperatures were investigated with commercial resin CHA-111 as reference. As shown in Fig. 8A, the adsorption isothermal model of PS-SBT at 293 K, 303 K and 313 K exhibited that high temperature was conducive to the adsorption of 1,3-propanediol. The adsorption capacity increased with the increase of temperature, indicating an endothermic process and the adsorption process was dominated by chemical adsorption.[30] PS-SBT and CHA-111 displayed striking difference in adsorption performance at 293 K, 303 K and 313 K. The adsorption performance of CHA-111 decreased with the increase of temperature, indicating that high temperature was not conducive to adsorption of 1,3-propanediol[40] and it was an exothermic process (the isothermal model of CHA-111 was shown in Fig. 8B).

As shown in Table 3, the Freundlich isothermal model is more suitable than Langmuir model for the adsorption performance of 1,3-propanediol by PS-SBT resin. Its correlation coefficient (R^2) is higher than that of Langmuir. The maximum adsorption capacity of PS-SBT at three temperatures is 117.698 mg g^{-1} at 293 K, 149.817 mg g^{-1} at 303 K and 184.620 mg g^{-1} at 313 K, respectively.

Adsorption enthalpy (ΔH, kJ mol^{-1}), adsorption free energy (ΔG, kJ mol^{-1}) and adsorption entropy (ΔS, J $(mol\ K)^{-1}$) are also discussed, and the transformation relationship among them can be described by the following equation:[24]

$$\ln C_e = \frac{\Delta H}{RT} + \ln K_F \quad (4)$$

$$\Delta G = -nRT \quad (5)$$

Table 3 Thermodynamic adsorption parameters towards 1,3-propanediol

		Langmuir model			Freundlich model		
Resin	Temperature (K)	Q_m (mg g^{-1})	K_L (L g^{-1})	R^2	K_F (mg^{1-n})	n	R^2
PS-SBT	293	117.698	0.047	0.994	8.085	1.524	0.998
	303	149.817	0.042	0.995	8.978	1.464	0.998
	313	184.620	0.042	0.995	10.925	1.452	0.997
CHA-111	293	420.402	0.011	0.997	5.238	1.134	0.997
	303	363.973	0.011	0.998	4.775	1.140	0.999
	313	305.315	0.012	0.998	4.148	1.132	0.996

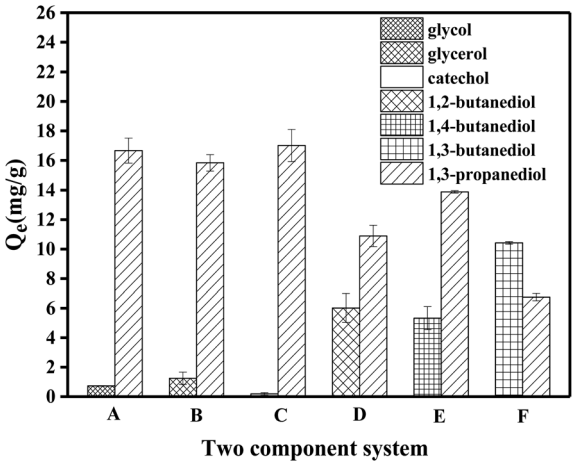

Fig. 9 Adsorption capacity of PS-SBT in a two-component system ((A) glycol + 1,3-propanediol; (B) glycerol + 1,3-propanediol; (C) catechol + 1,3-propanediol; (D) 1,2-butanediol + 1,3-propanediol; (E) 1,4-butanediol + 1,3-propanediol; (F) 1,3-butanediol + 1,3-propanediol).

$$\Delta S = \frac{(\Delta H - \Delta G)}{RT} \quad (6)$$

where R is the ideal gas constant (8.314 kJ (mol K)$^{-1}$); T (K) is the determined adsorption temperature; K_F and n is the corresponding characteristic constants in the Freundlich isotherm.

The ΔG, ΔH and ΔS of 1,3-propanediol adsorbed onto PS-SBT are listed in Table. S1.† It is seen that ΔG is negative, which implies the favorable and spontaneous adsorption process. The positive ΔH indicates that the adsorption is an endothermic process,[41] which is consistent with the isothermal adsorption model. The ΔH of 1,3-propanediol adsorbed onto boronic acid modified resin PS-SBT is calculated to need 0.5065 kJ mol^{-1} with the initial concentration of 1,3-propanediol from 1 g L^{-1} to 24 g L^{-1}. The positive ΔS reveals that more ordered structure of 1,3-propanediol is formed on the PS-SBT surface.

3.3.4 Competitive adsorption experiment. In order to better investigate the competitive adsorption in the 1,3-propanediol, we performed adsorption experiments on the two-component systems of different polyols and 1,3-propanediol, and the results were shown in the Fig. 9. The selectivity of PS-SBT towards glycol, glycerol and catechol was significantly lower than that of 1,3-propanediol, and the adsorption capacity of 1,3-propanediol was basically higher than 16 mg g^{-1} in the corresponding two-component systems. In order to further investigate the adsorption selectivity of polyols with similar structure, 1,2-butanediol, 1,3-butanediol and 1,4-butanediol were selected for the two-component adsorption experiment.

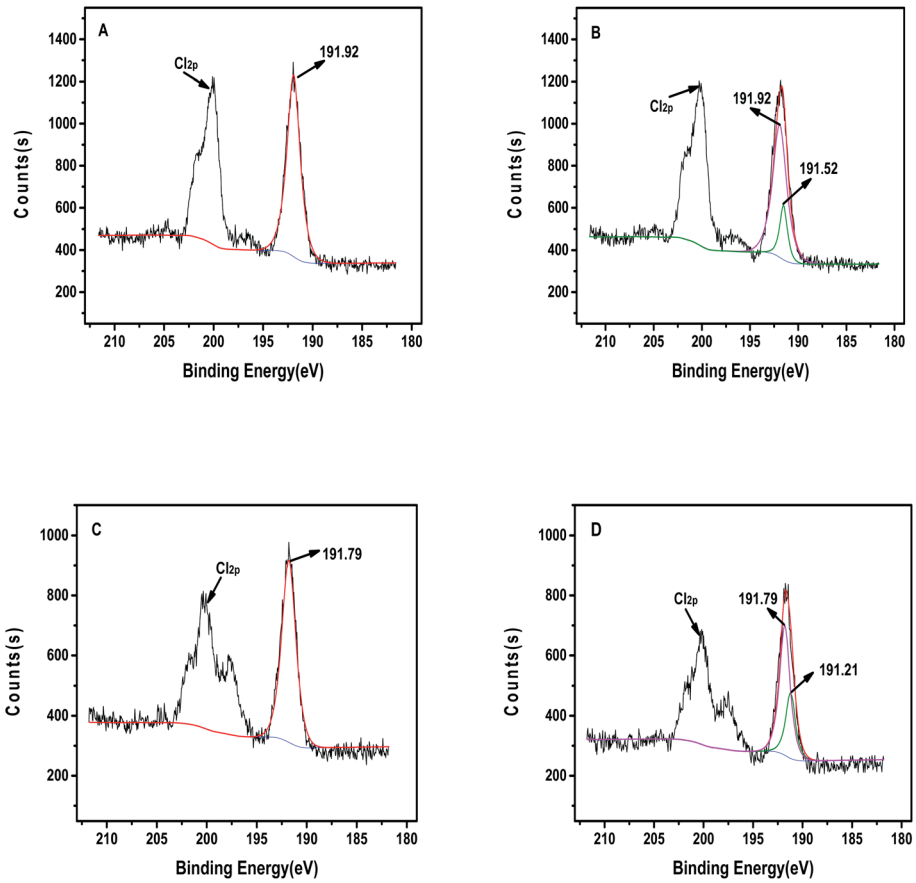

Fig. 10 XPS high resolution boron (B_{1s}) spectra of: (A) B_{1s} before adsorption 1,3-propanediol in PS-SBT; (B) B_{1s} after adsorption 1,3-propanediol in PS-SBT; (C) B_{1s} before adsorption 1,3-propanediol in PS-3NB; (D) B_{1s} after adsorption 1,3-propanediol in PS-3NB.

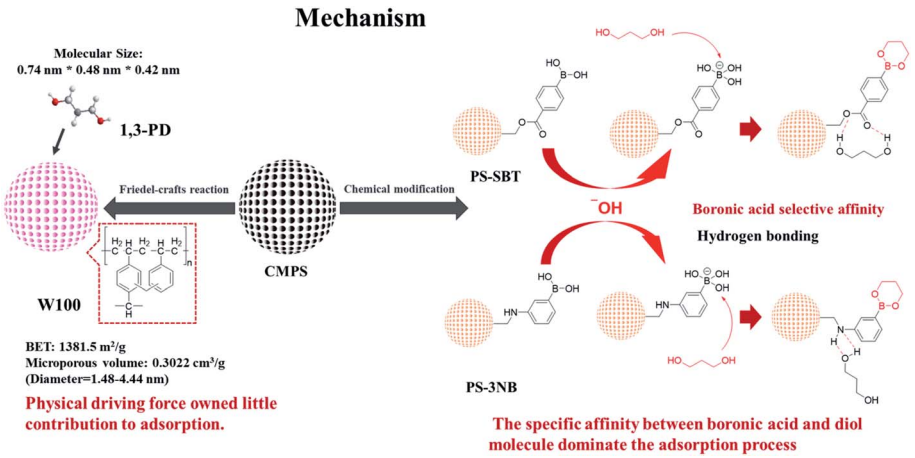

Fig. 11 Potential adsorption mechanism between modified resin and 1,3-propanediol.

The results showed that the selectivity of PS-SBT to 1,3-propanediol was higher than that of 1,2-butanediol and 1,4-butanediol, but the adsorption capacity decreased with the introduction of competitive adsorbents. It is worth noting that the adsorption capacity of 1,3-butanediol was higher than that of 1,3-propanediol, and the extension of carbon chain improved the affinity between 1,3-butanediol and PS-SBT, which might result from that 1,3-butanediol could generate relatively more stable five-membered borate with boronic acid than 1,3-propanediol. Therefore, PS-SBT generally exhibited a higher selectivity for 1,3-propanediol in the two-component competitive adsorption test and a structure-specific adsorption effect.

3.3.5 Regeneration and stability. The thermogravimetric analysis and adsorption–desorption cycle regeneration were performed to characterize the thermal stability and regeneration capability of the PS-SBT resin. The thermogravimetric analysis of boronic acid modified resin were shown in Fig. S2,† which showed that PS-SBT and PS-3NB still has a good structure at high temperature 573 K. As shown in Fig. S3,† there was no significant difference in adsorption capacity of 1,3-propanediol after six times of PS-SBT adsorption regeneration. The results show that boronic acid modified resin PS-SBT has a good regenerative adsorption effect on 1,3-propanediol.

3.3.6 Adsorption mechanism. The physical structure regulated resins and the chemical modified resins showed different adsorption forces during the adsorption process. PS-W and PS-S series physical resins mainly relied on intermolecular van der Waals forces to adsorb 1,3-propanediol. In the chemical modified resins, nitrogen and oxygen functional groups modified resins could generate hydrogen bonds and van der Waals forces with 1,3-propanediol, but the adsorption interaction forces with 1,3-propanediol were poor. Boronic acid modified resins could not only form hydrogen bond with 1,3-propanediol, van der Waals force, but also generated the specific boronic acid-diol molecules, which was quite favorable for the adsorption of 1,3-propanediol.

We performed XPS characterization analysis to clearly show the difference in binding energy before and after adsorption of boronic acid resin. Fig. 10A and B showed B_{1s} peak at about 191.92 eV before adsorption in PS-SBT resin, and a new peak appeared at 191.52 eV after adsorption, which may be caused by specific binding of boronic acid and diol structure. At the same time, the binding energy of boron in PS-3NB also changed before and after adsorption in Fig. 10C and D, and two peaks appeared in boron after adsorption, which were located at 191.21 and 191.79 eV, respectively. This indicated that the boron functional group participated in the adsorption process, and the electron cloud density around boron changed after adsorption, thus confirming the specific binding of boronic acid and diol structure. And after PS-3NB resin adsorbed 1,3-propanediol, the binding energy of nitrogen element in Fig. S4† appeared two peaks at 399.57 and 399.51 eV, and a new peak appeared at 399.51 eV after adsorption, which may be caused by hydrogen bonding generated.

The adsorption processes of PS-SBT, PS-3NB to 1,3-propanediol are pH-dependent process. In aqueous media, boronic acid exists as a balance of the neutral trigonal state and the anionic tetrahedral state which could generate boronate ester with 1,3-pronanediol, respectively.[42,43] Meanwhile, the neutral state boronate ester tends to hydrolyze reversibly to boronic acid. In contrary, the anionic tetrahedral state boronic acid could remain stable boronate ester (Fig. 11). Consequently, the introduction of hydroxyl ion could promote the reaction balance to shift to the stable anionic boronate ester and benefits the specific adsorption process. Besides, the optimal pH is related to the pK_a of the polyol and boronic acid.[44,45] According to the adsorption behaviors of PS-SBT and PS-3NB, the optimal pH was 10 and 14, respectively. Furthermore, the FT-IR before and after adsorption of PS-SBT modified resin revealed that the characteristic peak of B–O bond at 1373–1345 cm^{-1} existed and vibration band of C–O–C at 1145 cm^{-1} generated after adsorption in the solution pH of 10 (Fig. S5†).

4 Conclusions

In this paper, a series of physical structure regulation and chemical functional group modification resins were designed and synthesized on basis of chloromethyl polystyrene

divinylbenzene resin, and the adsorption process of 1,3-propanediol was systematically studied. Although the physical regulation resins were regulated with accurately specific surface area and pore structure through temperature and time factors, the adsorption affinity of 1,3-propanediol based on molecular size and other physical interactions was poor. The chemical modified resins with nitrogen and oxygen functional groups modification exhibited certain adsorption capacity for 1,3-propandiol which were only 71.9% and 29.3% of commercial resin CHA-111. The boronic acid modified resins exhibited effectively 1,3-propanediol adsorption affinity. The highest adsorption capacity between PS-SBT and 1,3-propanediol reached to 17.23 mg g^{-1}, which is 35% higher than that of commercial resin CHA-111. The further study demonstrated that the boronic acid content was positively correlated with the adsorption capacity, and the boronic acid content of PS-SBT was up to 1.220 mmol g^{-1}. The effect of boronic acid modified resin on the adsorption of pH in aqueous medium was also discussed. It was indicated that the adsorption capacity of PS-3NB to 1,3-propanediol was 37% higher than CHA-111 when pH was 14, and the excellent resin structure of PS-SBT might be destroyed. It illustrated that stability of resin and affinity with adsorbates are different in different pH media and laid the material foundation for the selective separation of polyols compounds.

Conflicts of interest

There are no conflicts to declare.

Acknowledgements

The authors gratefully acknowledge the generous support provided by Taishan Scholars Project of Shandong (No. ts201712076), Qingdao Original Innovation Program Basic Research for Application Project (18-2-2-47-jch).

References

1 R. Mishra, S. R. Jain and A. Kumar, *Biotechnol. Adv.*, 2008, **26**(4), 293–303.
2 C. Cui, Z. Zhang and B. Chen, *Bioresour. Technol.*, 2017, **245**(Pt A), 477–482.
3 K. Prochaska, J. Antczak, M. Regel-Rosocka and M. Szczygiełda, *Sep. Purif. Technol.*, 2018, **192**, 360–368.
4 Z. Li, L. Yan, J. Zhou, X. Wang, Y. Sun and Z.-L. Xiu, *Sep. Purif. Technol.*, 2019, **209**, 246–253.
5 Z. Wang, Z. Wu and T. Tan, *Biotechnol. Bioprocess Eng.*, 2013, **18**(4), 697–702.
6 M. C. S. Gomes, N. C. Pereira and S. T. D. Barros, *J. Membr. Sci.*, 2010, **352**(1–2), 271–276.
7 J. Saleh, A. Y. Tremblay and M. A. Dubé, *Fuel*, 2010, **89**(9), 2260–2266.
8 M. Naushad, A. A. Alqadami, Z. A. AlOthman, I. H. Alsohaimi, M. S. Algamdi and A. M. Aldawsari, *J. Mol. Liq.*, 2019, **293**, 111442.
9 P. Ma, S. Wang, T. Wang, J. Wu, X. Xing and X. Zhang, *Environ. Sci. Pollut. Res. Int.*, 2019, **26**(29), 30119–30129.
10 M. Guisnet and J. P. Gilson, *Zeolites for Cleaner Technologies Catalytic Science Series,* Imperial College Press, London, 2002.
11 A. Brito, M. E. Borges and N. Otero, *Energy Fuels*, 2007, **21**, 3280–3283.
12 L. Yang, L. Kong, H. Shi, M. Gu, S. Qin, Z. Shen, W. Zhang and Y. Zhang, *J. Fuel Chem. Technol.*, 2018, **45**(1), 48–54.
13 Y. Wang, N. Liu, H. Li and J. Liu, *Inorg. Chem. Ind.*, 2019, **51**(8), 60–63.
14 D. Liu, Y. He, C. Zhang and L. Zhang, *Funct. Mater.*, 2011, **5**(42), 721–723.
15 L. Cheng, Y. Zhang, Y. Li, L. Li and S. Sun, *Journal of Jilin University of Chemical Technology*, 2018, **35**(7), 48–52.
16 Y.-X. Jia, W. Sun, C. Yin, C. Xu, S. Yu and M. Xian, *J. Chem. Technol. Biotechnol.*, 2019, **94**(4), 1259–1268.
17 C. Long, Z. Lu, A. Li, W. Liu, Z. Jiang, J. Chen and Q. Zhang, *Sep. Purif. Technol.*, 2005, **44**(2), 115–120.
18 V. A. Davankov, S. V. Rogozhin and M. P. Tsyurupa, *US Pat.*, 3729457, 1971.
19 R. Xing, F. Liu, Z. Fei, J. Chen, Q. Zhang and A. Li, *Ion Exch. Adsorpt.*, 2006, **22**(4), 330–338.
20 Z. Fu, H. Li, L. Yang, H. Yuan, Z. Jiao, L. Chen, J. Huang and Y.-N. Liu, *Chem. Eng. J.*, 2015, **273**, 240–246.
21 C.-G. Oh, J.-H. Ahn and S.-K. Ihm, *React. Funct. Polym.*, 2003, **57**(2–3), 103–111.
22 G. Xiao and L. Long, *Appl. Surf. Sci.*, 2012, **258**(17), 6465–6471.
23 W. Yu, C. Xu, C. Yin, S. Yu, W. Sun, C. Xie and M. Xian, *Water Sci. Technol.*, 2018, **78**(10), 2096–2103.
24 J.-H. Huang, K.-L. Huang, S.-Q. Liu, A. T. Wang and C. Yan, *Colloids Surf., A*, 2008, **330**(1), 55–61.
25 Y. Ma, Q. Zhou, A. Li, C. Shuang, Q. Shi and M. Zhang, *J. Hazard. Mater.*, 2014, **266**, 84–93.
26 X. Wang, X. Yuan, S. Han, H. Zha, X. Sun, J. Huang and Y.-N. Liu, *Chem. Eng. J.*, 2013, **233**, 124–131.
27 X. Wang, R. Deng, X. Jin and J. Huang, *Chem. Eng. J.*, 2012, **191**, 195–201.
28 C. He, K. Huang and J. Huang, *J. Colloid Interface Sci.*, 2010, **342**(2), 462–466.
29 W. Yu, W. Sun, C. Xu, C. Wang, Y. Jia, X. Qin, C. Xie, S. Yu and M. Xian, *J. Taiwan Inst. Chem. Eng.*, 2018, **89**, 105–112.
30 X. Wang, J. Huang and K. Huang, *Chem. Eng. J.*, 2010, **162**(1), 158–163.
31 D. Štefanec and P. Krajnc, *React. Funct. Polym.*, 2005, **65**(1–2), 37–45.
32 A. Li, Q. Zhang, G. Zhang, J. Chen, Z. Fei and F. Liu, *Chemosphere*, 2002, **47**, 981–989.
33 S. K. Alamsetti and G. Sekar, *Chem. Commun.*, 2010, **46**(38), 7235–7237.
34 C. Yin, C. Xu, Y. X. Jia, W. Z. Sun, C. H. Wang, G. Z. Zhou and M. Xian, *J. Taiwan Inst. Chem. Eng.*, 2019, **95**, 383–392.
35 S. P. A. Hinkes and C. D. P. Klein, *Org. Lett.*, 2019, **21**(9), 3048–3052.
36 T. Nichele, C. Favero and A. Monteiro, *Catal. Commun.*, 2009, **10**(5), 693–696.

37 T. E. Pennington, C. Kardiman and C. A. Hutton, *Tetrahedron Lett.*, 2004, **45**(35), 6657–6660.
38 P. Leszczyński, T. Hofman and A. Sporzyński, *J. Solution Chem.*, 2020, **49**(6), 814–824.
39 B. Liu, J. Liu, D. Huang, J. Wei and D. Di, *Colloids Surf., A*, 2020, **595**, 124674.
40 X. Qiu, N. Li, X. Ma, S. Yang, Q. Xu, H. Li and J. Lu, *J. Environ. Chem. Eng.*, 2014, **2**(1), 745–751.
41 S. Chowdhury, R. Mishra, P. Saha and P. Kushwaha, *Desalination*, 2011, **265**(1–3), 159–168.
42 B. L. A. William and S. S. Brent, *Chem. Rev.*, 2016, **116**(3), 1375–1397.
43 G. Springsteen and B. Wang, *Tetrahedron*, 2002, **57**, 5291–5300.
44 J. Yan, G. Springsteen, S. Deeter and B. Wang, *Tetrahedron*, 2004, **60**(49), 11205–11209.
45 Q. Meng, J. Yu, L. Yang, Y. Li, M. Xian and H. Liu, *Sep. Purif. Technol.*, 2020, 117728.
46 L. Carlitz, *Duke Math. J.*, 1973, **40**(4), 893–901, DOI: 10.1215/S0012-7094-73-04083-0.